A Novel Approach to Realizing Low-Cost Plasmonic Optical Fiber Sensors: Light-Diffusing Fibers Covered by Thin Metal Films

Nunzio Cennamo *, Luigi Zeni, Francesco Arcadio, Ester Catalano and Aldo Minardo

Department of Engineering, University of Campania "L. Vanvitelli", via Roma n.29, 81031 Aversa, Italy; luigi.zeni@unicampania.it (L.Z.); francesco.arcadio@unicampania.it (F.A.); ester.catalano@unicampania.it (E.C.); aldo.minardo@unicampania.it (A.M.)
* Correspondence: nunzio.cennamo@unicampania.it; Tel.: +39 0815010367

Abstract: We have investigated, in a numerical and experimental way, a refractive index (RI) sensor based on surface plasmon resonance (SPR) in a silver-coated light-diffusing fiber (LDF). The experimental tests were conducted using water-glycerine mixtures with refractive indices ranging from 1.332 to 1.388. In the considered refractive index range, the experimental results show a sensitivity of the SPR wavelength to the outer medium's RI ranging from ~2600 to ~4700 nm/RIU, which is larger than the sensitivity recently reported for a gold-coated LDF sensor (~1200 to ~4000nm/RIU). The silver-coated sensor is also shown to ensure a higher signal-to-noise ratio (SNR) compared to the gold-coated sensor.

1. Introduction

An efficient optical sensing technique used to measure the refractive index (RI) of a dielectric medium (liquid media) in contact with a metal film is surface plasmon resonance (SPR). The technique exploits the interaction between free electrons of a metallic film and light, at the metal-dielectric interface. In SPR sensors, a high sensitivity can be obtained by the use of a silver (Al) or gold (Au) film. These metals, in particular the gold, are chemically stable and can be used in biochemical applications. Fiber-optic SPR sensors present several advantages, such as a low cost and small size, high performances, a very low sample volume, remote sensing capabilities, portability, and miniaturization. The small size of fiber-optic SPR sensors allows them to be incorporated into a multiple-fiber detection platform for the concurrent measurement of various components, such as different bio-chemical substances. In fact, efficient biosensors can be realized by immobilizing a bio-chemical receptor over the surface of an optical fiber SPR platform. These biosensors have been broadly studied [1–7]. Several variations have been introduced by exploiting different types of fibers and/or different manufacturing processes, in an effort to achieve an optimum sensitivity of the SPR sensor platform [8–14].

Excitation at the interface between a metal film and the surrounding medium of a superficial plasma wave requires access to the light propagating in the optical fiber [13]. In single-mode optical fibers, this usually requires the removal of the cladding by chemical etching, which raises production costs and affects the robustness of the sensor platform. In multimodal optical fibers with a silica core and polymer coating (the so-called hard-clad fibers), the cladding is easily removed using mechanical tools. However, SPR multimode sensors show a strong dependence of the SPR wavelength on the incidence angle of the incoming light [7,12].

We have recently demonstrated that a light-diffusing fiber (LDF), covered with a thin gold film, can be successfully employed as an SPR sensor platform [15]. Light-diffusing fibers have been designed with scattering centers in the core, leading to efficient light scattering through the sides of the optical fiber and along its length. Thanks to random scattering, the SPR phenomenon of an LDF is essentially independent of the incidence angle of the excitation light [15].

In SPR sensors, the thickness of the metal film or the metal material can generally be adjusted, according to the range of refractive indices to be detected. In the following, we report the results of an SPR sensor fabricated by sputtering a thin silver film above the uncoated area of the same LDF used in Ref. [15]. Comparing the new results with those achieved for the gold-coated SPR sensor, we show that the silver-coated sensor is more sensitive to RI changes and exhibits a higher SNR than the gold-coated sensor.

2. SPR Sensor Based on a Light-Diffusing Fiber

Figure 1 shows the host platform, based on a light-diffusing fiber (Fibrance® by Corning®, New York, NY, USA) formed by low-index polymeric cladding with a diameter of 230 μm, and a core of silica with a diameter of 170 μm [16] . This fiber has a nominal numerical aperture (NA) of >0.5, and the guided light is scattered radially outward, as reported in Figure 1b, through helical voids in random manner distributed along the core and wrapped around the axis of the fiber. In addition, the amount of scattered light is controlled by the pitch of the helical voids, with smaller pitches scattering more light than larger pitches. In our sample, the pitch is such that 90% of incoming light is scattered outside the fiber within the first 10 meters. The void diameter varies from 50 to 500 nm, scattering the light almost independently of its wavelength [16].
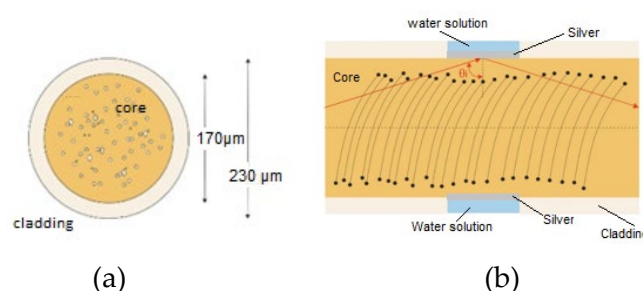

(a)   (b)

Figure 1. (**a**) LDF cross-section; (**b**) LDF lateral view with the portion of the sensing region.

The SPR sensor was fabricated by the use of a Miller stripping tool to remove the cladding along a 2-cm length of the fiber. Then, the unclad portion of the LDF was coated with a thin silver film, through sputter-coating (Bal-Tec SCD 500, Bal-tec AG, Balzers, Liechtenstein). Compared to gold, silver has lower ohmic losses, resulting in a narrower SPR line width [17]. In order to metalize the whole fiber circumference, the sputtering process was repeated twice, upon rotating the fiber by 180°. The deposited silver film had a nominal thickness of 50 nm. The silver film thickness was controlled by setting, on the sputter coater, the sputtering time and deposition rate. Furthermore, it was verified by comparing the experimental SPR spectra with numerical computations. In fact, the metal thickness has a strong influence on the minimum of the transmission spectrum, i.e., the transmissivity at the SPR wavelength. Therefore, the minimum of the transmission spectrum is indicative of the thickness of the deposited film.

Silver metal presented good adhesion to the core, as proved by its resistance to rinsing in de-ionized water. Figure 2 shows that the SPR-LDF sensor system comprises a tungsten halogen light source (HL2000, Ocean Optics, Dunedin, FL, USA), and a spectrometer with a detection range from 350 to 1000 nm (FLAME-S-VIS-NIR-ES, Ocean Optics, Dunedin, FL, USA). The light emitted by the tungsten lamp is coupled to the light diffusing fiber, while the transmitted light is analyzed through the spectrometer. The transmission spectrum of the fabricated sensor has been recorded while varying

the surrounding refractive index (SRI) using water-glycerol mixtures at different concentrations. An Abbe refractometer (model RMI by Exacta Optech, Germany) with a precision of 0,001 was used to measure the RI of each prepared mixture.
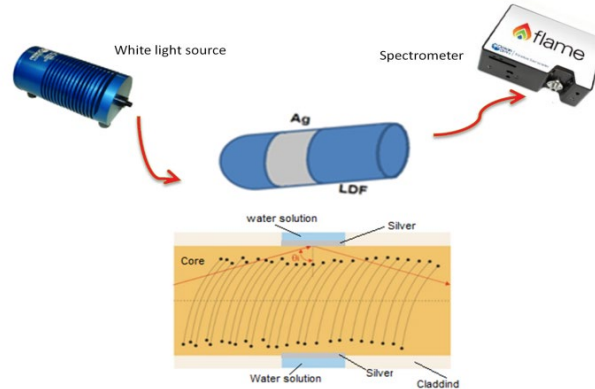

Figure 2. SPR-LDF sensor outline: sensing region with the experimental setup.

3. Results and Discussion

For these multimode fibers, a ray-optic description of light transmission through a fiber can be used in order to compute the power transmitted through the LDF [15]. According to this model, each optical ray propagating over a sensing length L experiences an amount of optical loss, depending on the reflection coefficient at the core-cladding interface and the number of reflections. As both these quantities depend on the propagation angle, by summing the power contributions over all the acceptance angles $(\theta_c, \pi/2)$, the power is calculated, where $\theta_c = sin^{-1}(n_{cl}/n_{c0})$) is the critical angle outside the region of the sensing. So, assuming non-polarized light, the results for the p-polarization and s-polarization must be averaged. Therefore, the normalized transmitted power is [18]

$$P_L = \frac{1}{2}\left(\frac{\sum_{\theta_i=\theta_c}^{\pi/2} P_0(\theta_i) \cdot R_p(\theta_i)^{N(\theta_i)}}{\sum_{\theta_i=\theta_c}^{\pi/2} P_0(\theta_i)} + \frac{\sum_{\theta_i=\theta_c}^{\pi/2} P_0(\theta_i) \cdot R_s(\theta_i)^{N(\theta_i)}}{\sum_{\theta_i=\theta_c}^{\pi/2} P_0(\theta_i)}\right) \tag{1}$$

where $P_0(\theta_i)$ is the initial power propagated by total internal reflection (TIR), $N(\theta_i) = cot(\theta_i)L/d$ is the number of reflections, and d is the diameter of the core; whereas R_p and R_s, for p-polarization and s-polarization, respectively, are the Fresnel reflectance coefficients at the boundary between the sensing medium (liquid medium) and the core. The Fresnel coefficients are deduced from the multi-layer structure formed by the fiber core, the metal layer, and the surrounding medium. When multimode optical fibers are illuminated by a lens with an NA greater than that of the fibers, in the fibers the power distribution among the different modes can be described with a Lambertian distribution [18]. However, in the case of light-diffusing fibers, a more accurate assumption is a perfectly scrambled angular distribution ($P_0(\theta_i) = const$ in Equation (1)) [15], due to the scrambling of optical energy operated by exploiting the helical voids running along the core.

Figure 3a,b show the experimental and numerical transmission spectra of the prepared sample. Each spectrum was obtained through normalization to the reference spectrum, acquired with air as the surrounding medium. As expected, both numerical and experimental spectra exhibit shorter SPR resonance wavelengths, compared to those achieved with the gold-coated sensor [15]. In particular, the SPR wavelength measured at $n_{sm} = 1.332$ is $\approx$ 570 nm, against an SPR wavelength of $\approx$630 nm measured with the gold-coated sample. In addition, a fine agreement between experimental and numerical spectra, in terms of minimum transmittance, is observed. In fact, except for the

measurement in water (n_{sm} = 1.332), in all other cases, the minimum transmittance is around 75%, in good agreement with simulations.
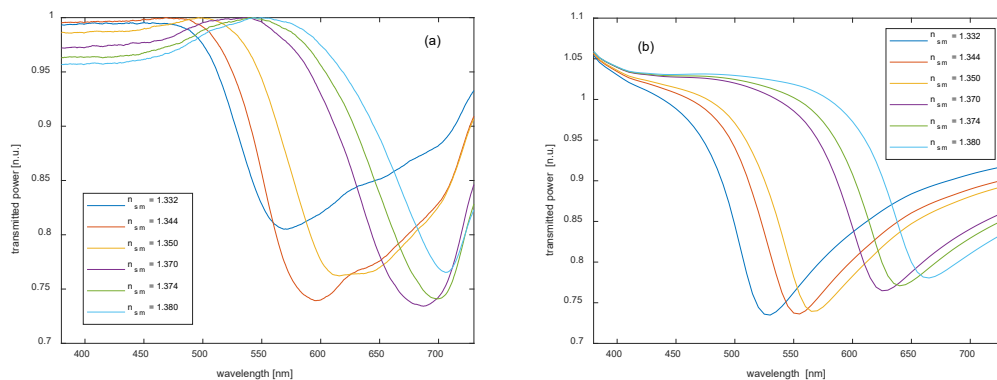

Figure 3. SPR spectra of the silver-coated sensor, after normalization to the transmission spectrum in air: (**a**) Experimental results; (**b**) numerical results.

From the spectra shown in Figure 3, we can deduce the SPR resonance wavelengths, i.e., the wavelengths related to the minimum of the transmitted power. The experimental and numerical SPR wavelengths are compared in Figure 4. We see that, while the experimental sensitivity (the SPR wavelength shift per unit change in RI) is in good agreement with simulations, the experimentally determined SPR wavelengths are always higher than those computed numerically. In particular, for n_{sm} = 1.332 the experimental data indicate an SPR wavelength of ≈570 nm, while numerical simulations provide an SPR wavelength of ≈530 nm. The discrepancy in the location of the SPR absorption peak may be caused by some non-uniformity of the metal thickness, or even roughness of the metal surface [19]. We also underline that, while the numerical model implies a scattering of the LDF independent of wavelength, the actual behavior may be different. As no exact modeling of the LDF light scattering dependence on wavelength is available, experimental characterization is necessary when moving from gold [15] to silver as the SPR metal, as different wavelength ranges are involved.
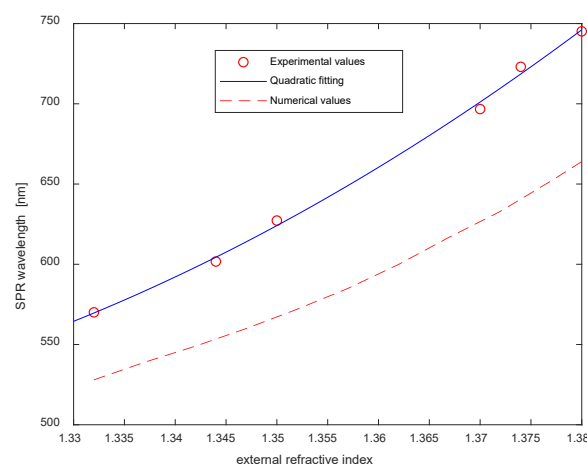

Figure 4. Resonance wavelength as a function of the surrounding refractive index: the circles are obtained from experimental data, and the dashed line is the result of numerical computations, while the quadratic fitting curve of the experimental values is reported by the continuous blue line.

As regards sensitivity, the quadratic fitting curve permits us to extrapolate a sensitivity ranging from 2600 nm/RIU (at $n_{sm} = 1.332$) to 4700 nm/RIU (at $n_{sm} = 1.380$).

Finally, it is worth comparing, at least for a couple of SRI values, the performance of the silver-coated sensor with that of the gold-coated sensor in terms of the signal-to-noise ratio (SNR) and sensitivity (S). Let us recall that SNR is defined as the SPR wavelength shift ($\Delta\lambda_{SPR}$) for a prescribed RI change, normalized to the full-width-at-half-maximum (FWHM) of the SPR curve ($\Delta\lambda_{FWHM}$), whereas the sensitivity is defined as the resonance wavelength shift per unit change in RI. Therefore, sensitivity and SNR equations are as follows [15]:

$$ S = \frac{\delta\lambda_{SPR}}{\delta n_{sm}} \left[\frac{nm}{RIU}\right] \tag{2} $$

$$ SNR = \frac{\Delta\lambda_{SPR}}{\Delta\lambda_{FWHM}} \tag{3} $$

Where λ_{SPR} is the resonance wavelength and n_{sm} is the surrounding refractive index. We compare in Table 1 the sensitivity and SNR of the silver-coated and gold-coated sensors, as derived from Equation (2), Equation (3), and the experimental data at $n_{sm} = 1.332$ and $n_{sm} = 1.350$. The reported values indicate that the silver-coated sensor not only has a higher sensitivity than the gold-coated sensor, but also exhibits a better SNR at both refractive indices.

Table 1. Comparison of performances, for two refractive indices (1.332 and 1.350), of silver-coated and gold-coated SPR LDF sensors.

Sensor Configuration	n_{sm}	Resonance Wavelength (λ_{SPR}) [nm]	Sensitivity (S) [nm/RIU]	SNR ($\Delta n_{sm} = 0.015$)
Silver-coated LDF	1.332	570	2640	0.21
Silver-coated LDF	1.350	627	3400	0.33
Gold-coated LDF [15]	1.332	629	1180	0.12
Gold-coated LDF [15]	1.350	658	2100	0.17

5. Conclusions

We have shown that efficient SPR refractive index sensors can be realized by deposing a thin silver film over a short length of an uncoated light-diffusing fiber. Compared to the gold-coated SPR sensor described in Ref. [15], the silver-coated sensor provides a higher sensitivity (2640 nm/RIU vs 1180 nm/RIU at $n_{sm} = 1.332$) and better SNR (0.21 vs 0.12 at $n_{sm} = 1.332$). Besides providing a high sensitivity, the tested plasmonic sensor does not require complex and expensive manufacturing of the fiber. Only the metallization of the sensing area is required. The developed sensor is repeatable and is suitable for real-time detection. Therefore, it could be used with different kinds of receptors for biochemical sensing applications.

While this paper represents the first comparative analysis between silver and gold SPR sensors based on an LDF platform, several previous analyses have led to the conclusion that silver-based SPR sensors exhibit enhanced sensitivity and narrower SPR resonance, compared to SPR sensors based

on a gold film [20–24]. However, it is also true that silver is less chemically stable than gold, which makes it less appealing for biosensing applications. A possible solution may consist of using a multilayered film such as a bimetallic Au/Ag thin film [17], or a tri-layered metallic structure [21], which combines the enhanced SPR features of silver with the chemical stability of gold.

References

1. Homola, J. Present and future of surface plasmon resonance biosensors. *Anal. Bioanal. Chem.* **2003**, *377*, 528–539.

2. Homola, J.; Yee, S.S.; Gauglitz, G. Surface plasmon resonance sensors: review. *Sens. Act. B: Chem.* **1999**, *54*, 3–15.

3. Liu, Y.; Liu, Q.; Chen, S.; Cheng, F.; Wang, H.; Peng, W. Surface Plasmon Resonance Biosensor Based on Smart Phone Platforms. *Sci Rep.* **2015**, *5*, 12864.

4. Caucheteur, C.; Guo T.; Albert, J. Review of plasmonic fiber optic biochemical sensors: improving the limit of detection. *Anal. Bioanal. Chem.* **2015**, *407*, 3883–3897.

5. Klantsataya, E.; Jia, P.; Ebendorff-Heidepriem, H.; Monro, T.M.; François, A. Plasmonic fiber optic refractometric sensors: from conventional architectures to recent design trends. *Sensors* **2017**, *17*, 12.

6. Anuj, K.; Sharma, R.J.; and Gupta, B.D. Fiber-optic sensors based on surface Plasmon resonance: a comprehensive review. *IEEE Sens. J.* **2007**, *7*, 1118–1129.

7. Trouillet, A.; Ronot-Trioli, C.; Veillas, C.; Gagnaire, H. Chemical sensing by surface plasmon resonance in a multimode optical fiber. *Pure Appl. Opt.* **1996**, *5*, 227–237.

8. Pollet, J.; Delport, F.; Janssena, K.P.F.; Jans, K.; Maes, G.; Pfeiffer, H.; Wevers, M.; Lammertyn, J. Fiber optic SPR biosensing of DNA hybridization and DNA–protein interactions. *Biosens. Bioelectron.* **2009**, *25*, 864–869.

9. Masson, J.F.; Kim, Y.C.; Obando, L.A.; Peng, W.; Booksh, K.S. Fiber-optic surface plasmon resonance sensors in the near-infrared spectral region. *Appl. Spectrosc.* **2006**, *60*, 1241–1246.

10. Slavik, R.; Homola, J.; Ctyroky, J. Single-mode optical fiber surface plasmon resonance sensor. *Sens Actuators B Chem.***1999**, *54*, 74–79.

11. Jorgenson, R.C.; Yee, S.S. A fiber-optic chemical sensor based on surface plasmon resonance. *Sens. Actuators B Chem.* 1993, *12*, pp. 213–220, 1993.

12. Cennamo, N.; Massarotti, D.; Conte, L.; Zeni, L. Low Cost Sensors Based on SPR in a Plastic Optical Fiber for Biosensor Implementation. *Sensors* **2011**, *11*, 11752–11760, 2011.

13. Liang, G.; Luo, Z.; Liu, K.; Wang, Y.; Dai, J.; Duan, Y. Fiber Optic Surface Plasmon Resonance–Based Biosensor Technique: Fabrication, Advancement, and Application. *Crit. Rev. Anal. Chem.* **2016**, *46*, 213–223.

14. Galatus, R.; Farago, P.; Cennamo, N.; Cristea, C.; Feier, B. SPR based hybrid electro-optic biosensor platform: SPR-cell with side emitting plastic optical fiber. 2017 IEEE 23rd International Symposium for Design and Technology in Electronic Packaging (SIITME), Constanta, Romania, 2017, pp. 328-331

15. Cennamo, N.; Zeni, L.; Catalano, E.; Arcadio, F.; Minardo, A. Refractive Index Sensing through Surface Plasmon Resonance in Light-Diffusing Fibers. *Appl. Sci. vol.* **2018**, *8*, 1172.

16. Logunov, S.; Fewkes, E.; Shustack, P.; Wagner, F. Light Diffusing Optical Fiber for Illumination. In Renewable Energy and the Environment. Paper DT3E.4; OSA Technical Digest (online), Optical Society of America: Washington, DC, USA, 2013.

17. Hottin, J.; Wijaya, E.; Hay, L.; Maricot, S.; Bouazaoui, M.; Vilcot, J.-P. Comparison of Gold and Silver/Gold Bimetallic Surface for Highly Sensitive Near-infrared SPR Sensor at 1550 nm. *Plasmonics*, **2013**, *8*, 619.

18. Sharma, A.K.; Gupta, B.D. Absorption-based fiber optic surface plasmon resonance sensor: A theoretical evaluation. *Sens. Actuators B Chem.* **2004**, *100*, 423–431.

19. Kanso, M.; Cuenot, S.; Louarn, G. Roughness effect on the SPR measurements for an optical fibre configuration: experimental and numerical approaches, *J. Opt. A: Pure Appl. Opt.* **2007**, *9*, 586.

20. Li, Chung-Tien; Lo, Kun-Chi; Chang, Hsin-Yun; Wu, Hsieh-Ting; Ho, J.H.; Yen, Ta-Jen. Ag/Au bi-metallic film based color surface plasmon resonance biosensor with enhanced sensitivity, color contrast and great linearity. *Biosensors and Bioelectronics* **2002**, *36*, 192–198.

21. Xia, L.; Yin, S.; Gao, H.; Deng, Q.; Du, C. Sensitivity Enhancement for Surface Plasmon Resonance Imaging Biosensor by Utilizing Gold–Silver Bimetallic Film Configuration. *Plasmonics* **2011**, *6*, pp. 245–250.

22.　Lin, W. B.; Lacroix, M.; Chovelon, J.M.; Jaffrezic-Renault, N.; Gagnaire, H. Development of a fiber-optic sensor based on surface plasmon resonance on silver film for monitoring aqueous media. *Sensors Actuators B Chemical* **2001**, *75*, 203–209.

23.　Choi, Seung Ho; Kim, Y.L.; Byun, K.M. Graphene-on-silver substrates for sensitive surface plasmon resonance imaging biosensors. *Opt. Express* **2011**, *19*, 458–466.

24.　Wang, Z.; Cheng, Z.; Singh, V.; Zheng, Z.; Wang, Y.; Li, S.; Song, L.; Zhu, J. Stable and sensitive silver surface plasmon resonance imaging sensor using trilayered metallic structures. *Anal Chem.* **2014**, *86*, 1430–1436.